Optical dephasing in semiconductor mixed crystals

U. Siegner, D. Weber, E. O. Göbel, D. Bennhardt, V. Heuckeroth, R. Saleh, S. D. Baranovskii, and P. Thomas
Fachbereich Physik and Zentrum für Materialwissenschaften, Philipps-Universität, Renthof 5, D-3550 Marburg, Federal Republic of Germany

H. Schwab and C. Klingshirn
Fachbereich Physik der Universität, Erwin-Schrödinger-Strasse, D-6750 Kaiserslautern, Federal Republic of Germany

J. M. Hvam
Fysik Institut, Odense Universitet, Campusvej 55, DK-5230 Odense, Denmark

V. G. Lyssenko
Institut of Problems of Microelectronics Technology and Superpure Materials, Chernogolovka, Moscow district 142 432, Russian Federation
(Received 8 April 1992)

The influence of disorder and localization on optical dephasing of excitons in the semiconductor mixed crystals $CdS_{1-x}Se_x$ and $Al_xGa_{1-x}As$ has been investigated by means of time-resolved four-wave mixing and photon echo experiments. A dephasing time of several hundreds of picoseconds is found for resonantly excited localized excitons in $CdS_{1-x}Se_x$ while the dephasing time in $Al_xGa_{1-x}As$ amounts to only a few picoseconds. In $CdS_{1-x}Se_x$ dephasing results mainly from hopping processes, i.e., exciton-phonon interaction. The contribution of disorder is negligible in terms of phase relaxation in $CdS_{1-x}Se_x$. In contrast, in $Al_xGa_{1-x}As$ elastic disorder scattering yields an essential contribution to the dephasing rate. We present a theoretical model, which treats dephasing of optical excitations in a disordered semiconductor, including the influence of disorder as well as exciton-phonon interaction. On the base of this model, the experimentally observed differences in the dephasing behavior of excitons in $CdS_{1-x}Se_x$ and $Al_xGa_{1-x}As$ are related to the microscopic structure of the disorder potential and the mechanism of exciton localization.

I. INTRODUCTION

Solids characterized by static disorder have been a subject of interest for several decades. The pioneering work of Anderson[1] on "absence of diffusion in certain random lattices" has been followed by a steadily increasing number of studies investigating the critical behavior of transport properties of disordered media. The new feature of (infinite) disordered systems with degenerate statistics is the disappearance of conductivity at zero temperature although the single-particle spectrum is continuous at the Fermi level. This regime of nonconducting states is separated from the conducting states by the mobility edge E_b.[2] In terms of wave functions, the two regimes are also described by localized and extended states, respectively.

Besides the fundamental interest in localization as a critical phenomenon, research has also been stimulated by the more technical need to characterize the nature of disorder in a given system, such as amorphous semiconductors, mixed crystals, or heterostructures. In semiconductors with nondegenerate statistics, equilibrium transport experiments, however, do not give clear-cut information on disorder-induced effects since they have to be performed at rather high temperatures in order to have a sufficiently large density of carriers. Then the concept of localization becomes questionable due to phonon-assisted hopping transport processes and phonon-induced delocalization.[3-5] In addition, the transport data in this situation are given by a superposition of a wide spectrum of transport channels. At first sight, optical experiments seem to be more feasible to study the effect of disorder on electronic properties since they can be performed at low temperatures.

However, it can easily be demonstrated that linear optical spectra of disordered semiconductors cannot show critical behavior. Disorder merely induces a particular kind of Urbach tails at the fundamental band edge. These tail states are observed in linear absorption measurements. In photoluminescence experiments disorder manifests itself in an inhomogeneous broadening of the optical transitions. The inhomogeneous linewidth, however, cannot unambiguously be related to the detailed properties of the disorder potential.

Time-resolved photoluminescence experiments have been used to gain insight into the dynamics of optical excitations in disordered semiconductors.[6-9] In fact, these data can give information about energy relaxation within the localized states and thus about details of the single-particle spectrum and the interaction of localized excitations with phonons. The time-resolved photolumines-

cence spectra, however, are still determined by a superposition of various relaxation channels with extremely wide spectra of relaxation rates. More direct experimental probes are desirable in order to clarify the influence of disorder on the dynamics of optical excitations.

The availability of ultrashort laser pulses has offered the possibility of examining experimentally the very first steps in light-matter interaction. In this respect, experiments which monitor the irreversible decay of the initially generated macroscopic polarization in the disordered medium are of particular interest. This decay can be measured using transient degenerate four-wave-mixing (FWM) experiments, including stimulated and spontaneous photon echo experiments. Laser excitation of matter initially creates a coherent macroscopic polarization. Interaction of the excited individual species among each other and with their environment irreversibly destroys their fixed phase relation imprinted by the driving electric laser field and thus the macroscopic polarization. This is generally referred to as optical dephasing.

While it is plausible that every interaction process of an optical excitation with a bath of quasiparticles destroys the initially generated optical phase, the influence of static disorder on the polarization decay is less evident. Therefore, we have theoretically studied[10–12] the influence of disorder scattering on optical phase coherence in the absence of dynamical quasiparticle interaction. Since we are dealing with semiconductors, Coulomb interaction is an indispensable ingredient in any theory of optical dephasing.

Even though in recent years powerful many-body theories have been developed to fully describe interaction of laser light with ordered semiconductors,[13–21] from the point of view of a qualitative physical understanding in the case of disordered semiconductors it seems helpful to start from a different approach and to take into account the important and relevant processes step by step.

The most instructive model system to start with is an ensemble of two-level systems with dipole-allowed transitions between the ground and excited state. Intersite coupling among the upper and lower states leads to a conduction and a valence band, respectively. Disorder can easily be incorporated in the sense of diagonal disorder in this tight-binding model.

The analysis will show that in photon echo experiments critical behavior due to localization can be expected in principle in the long-time limit. This is due to the fact that the third-order nonlinear susceptibility contains configuration averages of the correlation of electron (and hole) propagation in the conduction (valence) band, very much like the Kubo formulation of conductivity. Since correlation of propagating amplitudes determines dephasing, Coulomb interaction must be taken into account for a realistic description. Our analysis shows that Coulomb interaction may stabilize the phases of optical excitations in a disordered semiconductor, which in certain cases can be explained by internal phase conjugation.

Besides the direct influence of disorder on phase relaxation, static disorder can cause localization of optical excitations. In turn, the quasiparticle interaction of localized excitations can be considerably modified as compared to free excitations in pure crystals. Thus, disorder can have both a direct and an indirect effect on dephasing: (i) directly via elastic scattering at the disorder potential, and (ii) indirectly because of the modification of quasiparticle scattering. The interpretation of experimental data thus requires an understanding of the interrelation of disorder-induced localization and quasiparticle interaction. It is the aim of this paper to discuss the underlying physical processes for a particular class of disordered semiconductors, namely II-VI and III-V mixed crystals, both theoretically and experimentally. In contrast to amorphous semiconductors, mixed crystals are characterized by weak static disorder. The crystalline lattice is still existent; only the distribution of one kind of the constituents, i.e., the anions and cations, on the lattice sites is random. As a consequence, excitons can still be assumed to be well-defined excitations. On the other hand, an intrinsic inhomogeneous optical transition has to be expected leading to a distinct echolike signal in the FWM experiment.

Experimentally we have investigated localized exciton transitions in $CdS_{1-x}Se_x$ and $Al_xGa_{1-x}As$ mixed crystals by means of time-resolved degenerate FWM and photon echo experiments. The contributions of the different scattering mechanisms to optical dephasing have been separated, thereby also obtaining information on elastic-scattering processes. We will show that in fact disorder-induced localization significantly affects optical dephasing of the excitonic excitations. In turn, our investigations point out that, in contrast to linear optical experiments, the study of optical dephasing may provide microscopic information on the nature of static disorder and localization in semiconductors and semiconductor microstructures.

In Sec. II of this paper, we review the relevant data on linear optical properties and particularly on the photoluminescence spectra of the disordered mixed crystals $CdS_{1-x}Se_x$ and $Al_xGa_{1-x}As$. We also briefly summarize the widely accepted picture of their electronic structure. In particular, we point out that the linear optical spectra show strong inhomogeneous broadening of the exciton transitions due to disorder.

Section III describes the experimental technique of time-resolved FWM and photon echo experiments, which have been employed to determine the optical dephasing rates. In this section, we also briefly discuss experimental results obtained for exciton dephasing in the binary semiconductors GaAs and CdSe, where disorder is absent.

The theoretical concept and model is presented in Sec. IV. We will begin with a discussion of the effect of disorder on dephasing of an ensemble of coupled two-level systems neglecting Coulomb interaction and phonons. Next the influence of disorder on optical dephasing of excitons will be discussed. Finally, we treat the effect of phonon coupling on dephasing in disordered semiconductors, taking into account local as well as nonlocal (hopping) interaction with phonons. In particular, we calculate the temperature dependence of the dephasing rate for a model describing the dynamics of localized excitons in II-VI mixed crystals.

The experimental results of the dephasing studies on

$CdS_{1-x}Se_x$ and $Al_xGa_{1-x}As$ are presented in Secs. V and VI, respectively. We have investigated the $CdS_{1-x}Se_x$ system in great detail, including the photon energy, excitation intensity, and temperature dependence of the optical dephasing time. It is demonstrated that the low-temperature dephasing times are considerably longer as compared to those of binary CdSe.[22,23] The dephasing times increase with increasing localization energy and decrease with increasing temperature. Yet, the analytic dependence of the dephasing time on temperature depends on the localization energy, in agreement with the prediction of our theoretical model.

The experimental results for $Al_xGa_{1-x}As$ presented in Sec. VI significantly differ from those obtained for $CdS_{1-x}Se_x$. The dephasing times are of the order of a few picoseconds, i.e., much shorter than in $CdS_{1-x}Se_x$. The dephasing times are comparable to the numbers reported for binary GaAs.[24,25] Consequently, disorder and localization have a different effect on dephasing in the $Al_xGa_{1-x}As$ system as compared to $CdS_{1-x}Se_x$ in spite of the very similar linear optical properties. On the basis of our theoretical model, we will discuss the implications of these results on the nature of disorder in these systems.

Finally, we summarize our present understanding of dephasing in disordered semiconductor mixed crystals in Sec. VII. We shall point out once again that nonlinear optical studies in general and optical dephasing experiments in particular may provide information on the detailed nature of disorder and the mechanisms of electronic localization in bulk semiconductors and also in semiconductor microstructures.

II. LINEAR OPTICAL PROPERTIES OF $CdS_{1-x}Se_x$ AND $Al_xGa_{1-x}As$ MIXED CRYSTALS

In this section, the linear optical properties of $CdS_{1-x}Se_x$ and $Al_xGa_{1-x}As$ are briefly reviewed. Beginning with the basic optical properties, which can also be found in the ordered binary compounds, we discuss in particular those features of linear optical spectra which are related to disorder. In fact, disorder and localization considerably change the linear absorption, reflection, and photoluminescence spectra of a semiconductor and, in turn, some information on disorder has already been obtained by linear optical experiments.

First we concentrate on $CdS_{1-x}Se_x$ mixed crystals. The basic optical properties of $CdS_{1-x}Se_x$ mixed crystals can be understood within the virtual crystal approximation, i.e., the model which assumes that all properties of a mixed crystal can be interpolated from the properties of the respective binary compounds. Beyond the virtual crystal approximation, however, disorder comes into play and leads to phenomena which cannot be observed in ordered semiconductors, e.g., localization of optical excitations and zero-phonon "nondirect" transitions.

In the virtual crystal approximation, $CdS_{1-x}Se_x$ is a direct-gap semiconductor, which crystallizes in the hexagonal wurtzite structure. The fundamental band gap is located at the center of the (virtual crystal) Brillouin zone. The band gap is continuously tunable between the band-gap energies of CdS and CdSe depending on composition. As a result of the predominantly ionic binding, the valence-band states mainly arise from the occupied p orbitals of the group-VI ions while the empty s orbitals of the cadmium ions form the conduction band. The degeneracy in the valence band is lifted by the combined action of spin-orbit coupling and an internal electric field, which results from the noncubic crystal symmetry.[26,27] Three nondegenerate valence bands are formed. As to the optical selection rules, we note that transitions involving the upper valence band are dipole allowed only if the excitation field is polarized perpendicularly to the optical axis.[28] The optical properties of direct-gap semiconductors close to the fundamental band gap are dominated by exciton transitions at low temperatures. This is particularly true in the case of $CdS_{1-x}Se_x$ since the exciton binding energy is rather large. The exciton binding energy is in the range between 15 meV (pure CdSe) and 29 meV (pure CdS),[29] depending on composition.

Beyond the virtual crystal approximation, disorder in $CdS_{1-x}Se_x$ mixed crystals arises from local variations of the concentration x, which leads to a spatially fluctuating crystal potential. In linear optical experiments, the fluctuations of the crystal potential manifest themselves in an inhomogeneous broadening of the exciton transition. The inhomogeneous broadening of the exciton line has been observed in reflection, absorption, and photoluminescence spectra,[30–33] from which inhomogeneous linewidths in the range 5–15 meV can be inferred. Finite absorption is observed below the band-gap energy obtained by the virtual crystal approximation. Thus, the density of states is modified by disorder, giving rise to tail states below the conduction-band edge and above the valence-band edge.[34,35] The precise shape of the density-of-states tail is difficult to determine experimentally. Often an exponentially decaying tail is assumed according to

$$g(\varepsilon) \propto \exp\left[-\frac{\varepsilon}{\varepsilon_0}\right], \tag{1}$$

where ε is the localization energy and ε_0 the tailing parameter (energy scale of the tail). The tailing parameter typically amounts to 5 meV for $CdS_{1-x}Se_x$.[36]

Exciton transitions in $CdS_{1-x}Se_x$ mixed crystals involve these tail states. Cohen and Sturge[31] and Permogorov *et al.*[32] have independently demonstrated by means of photoluminescence experiments that excitons in $CdS_{1-x}Se_x$ are localized in the potential wells of the fluctuating disorder potential. Exciton localization has experimentally been observed in $CdS_{1-x}Se_x$ mixed crystals with selenium concentrations x between 3% and 65%.[37] The concept of the mobility edge has also been applied to $CdS_{1-x}Se_x$ mixed crystals. Due to the finite temperature and the finite lifetime of excitons, the mobility edge has to be considered as an effective one, which separates delocalized band states from localized tail states. The spectral position of the effective mobility edge can be characterized referring to the photoluminescence spectrum for nonresonant, above-band-gap excitation. The mobility

edge is situated at the high-energy edge of the photoluminescence spectrum.[32,38] This result shows that the photoluminescence spectrum is dominated by localized exciton emission. Delocalized excitons are trapped in the localized states before they can recombine radiatively.

The dynamics of localized excitons in $CdS_{1-x}Se_x$ have been investigated directly in the time domain by time-resolved luminescence experiments.[6-9] As the most important result of these experiments, we note that energy relaxation within the tail states is considerably slower than in the extended states. At low temperatures, intraband energy relaxation in $CdS_{1-x}Se_x$ mixed crystals takes place via hopping processes, i.e., phonon-assisted spatial transfers of an exciton between two local minima of the fluctuating random potential. The typical time constant for a hopping process is in the range of a hundred picoseconds at low temperatures. At elevated temperatures, exciton dynamics is dominated by thermally activated multiple-trapping processes.

While $CdS_{1-x}Se_x$ has been studied comprehensively in terms of alloy disorder and exciton localization, the investigation of $Al_xGa_{1-x}As$ mixed crystals has mainly been restricted to photoluminescence studies.[39-46] Before we discuss the influence of disorder on the linear optical spectra of $Al_xGa_{1-x}As$, we briefly recall its basic optical properties within the framework of the virtual crystal approximation.

$Al_xGa_{1-x}As$ is a direct-gap semiconductor for aluminum concentrations less than about 45%.[47] The band gap is at the center of the Brillouin zone. As compared to $CdS_{1-x}Se_x$, binding in the III-V semiconductor is more covalent. This binding character leads to the fact that group-III-ion and group-V-ion orbitals contribute to both the valence-band and the conduction-band states. The aluminum ions and gallium ions are randomly distributed on the cation sublattice, resulting in a fluctuating disorder potential. Photoluminescence studies have shown an inhomogeneous broadening of the exciton transitions.[39-46] The width of the inhomogeneous line sensitively depends on the detailed conditions during the epitaxial growth of the $Al_xGa_{1-x}As$ layers. Theoretical studies predict an increase of the inhomogeneous broadening due to alloy disorder if the aluminum concentration is increased.[43,48-50] The experimental work reported in Refs. 43 and 45 verifies this prediction and it definitely demonstrates the inhomogeneous broadening to result from alloy disorder. Typical inhomogeneous linewidths in $Al_xGa_{1-x}As$ mixed crystals with 30–40 % of aluminum are of the order of 10 meV.

The problem of exciton localization has been investigated experimentally by Sturge, Cohen, and Logan[51] in indirect $Al_xGa_{1-x}As$ mixed crystals with an aluminum content of 55%. They have found evidence of localization of the indirect exciton at very low temperatures. To the best of our knowledge, localization of excitons has not yet directly been demonstrated in direct-gap $Al_xGa_{1-x}As$ mixed crystals.

Summarizing this section, we point out that linear optical experiments have revealed inhomogeneous broadening of the exciton transition due to compositional disorder both in $CdS_{1-x}Se_x$ and $Al_xGa_{1-x}As$ mixed crystals. In $CdS_{1-x}Se_x$ localization of excitons has been demonstrated while the question of exciton localization in direct-gap $Al_xGa_{1-x}As$ mixed crystals is still open. The detailed properties of the random disorder potential, however, cannot be addressed by linear optical experiments.

III. EXPERIMENT

Optical phase relaxation can be studied directly in the time domain by time-resolved degenerate FWM experiments.[52] The general setup of the experiment is schematically depicted in Fig. 1. Three coherent laser pulses with equal frequencies and wave vectors $\mathbf{k}_1, \mathbf{k}_2$, and $\mathbf{k}_3$, respectively, are employed to excite an optical transition of a sample. The three pulses are time delayed with respect to each other. We refer to the time delay between pulse no. 1 and pulse no. 2 as t_{21} while pulse no. 2 and pulse no. 3 are delayed by a time t_{23}. Third-order nonlinear interaction in the sample generates a signal which is emitted in the phase-matching direction $\mathbf{k}_4=\mathbf{k}_3+\mathbf{k}_2-\mathbf{k}_1$. The time evolution of the FWM signal and the physical processes which give rise to the signal, however, depend on the nature of the excited optical transition.

For homogeneously broadened transitions, the macroscopic polarization induced by pulse no. 1 is converted into a population grating by the second pulse. The diffraction efficiency of this grating can be probed by pulse no. 3. The diffracted light represents the FWM signal. The FWM signal is emitted instantaneously after the application of pulse no. 3. The intensity of the signal as a function of the time delay t_{21} depends on the rate of scattering processes, which irreversibly destroy the phase coherence among the induced dipole moments and thus the macroscopic polarization. As a consequence, the amplitude of the population grating and its diffraction efficiency decrease. The irreversible decay of phase coherence due to scattering is referred to as optical dephasing and described by the phase relaxation time T_2.

For inhomogeneously broadened transitions, the different frequencies excited within the inhomogeneous line give rise to destructive interference between polariza-

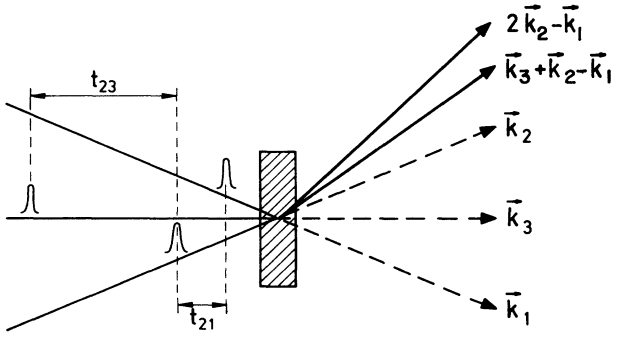

FIG. 1. Schematic diagram of a time-resolved four-wave-mixing (FWM) experiment. The time delays t_{21} and t_{23} between the excitation pulses are indicated. The three-pulse FWM signal and the two-pulse FWM signal are emitted in the directions $\mathbf{k}_3+\mathbf{k}_2-\mathbf{k}_1$ and $2\mathbf{k}_2-\mathbf{k}_1$, respectively.

tion components which have acquired different phases according to their local frequencies. The destructive interference causes a decay of the macroscopic polarization with a time constant roughly equal to the inverse of the excited inhomogeneous linewidth, even in the absence of any scattering.

This interference decay, however, can be reversed by application of pulse no. 2, which produces a phased array, i.e., a distribution of phase-shifted population gratings, each of them corresponding to a certain frequency. Pulse no. 3 stimulates radiation from the phased array such that constructive interference takes place after a time delay equal to the time delay t_{21} between pulse no. 1 and pulse no. 2. Thus, the FWM signal is emitted time delayed with respect to the stimulating pulse as a result of the inhomogeneous broadening.[53] This phenomenon is usually referred to as stimulated photon echo.

The intensity of the stimulated photon echo decays as a function of t_{21} due to optical phase relaxation and thus allows us to determine the phase relaxation time T_2 according to the relation

$$I_{\text{echo}} \propto \exp\left[-\frac{t_{21}}{T_2/4}\right] \tag{2}$$

if the decay is purely exponential.

In addition, stimulated photon echo experiments are a powerful tool to investigate energy relaxation.[53] The intensity of the stimulated photon echo pulse also depends on the time delay t_{23} and the population decay time constant. The population decay time constant includes recombination, diffusion, and intraband energy relaxation provided that the time delay t_{21} is larger than the pulse duration. The sensitivity to energy relaxation results from the fact that the phase shifts acquired by the individual oscillators in the time interval t_{21} can be compensated only if the local frequencies of all oscillators remain unchanged during the experiment. The recombination time T_1 and the influence of diffusion can independently be determined studying the decay of an ordinary population grating,[54] where pulse no. 1 and pulse no. 2 coincide in time ($t_{21}=0$). Thus, a comparison of the phased array decay to the population grating decay yields the energy relaxation time T_3.

Finally, we note that besides the three-pulse FWM signal discussed so far, a two-pulse FWM signal is generated and emitted in the direction $2\mathbf{k}_2-\mathbf{k}_1$. This signal can be considered as a special case of the three-pulse signal with $\mathbf{k}_2=\mathbf{k}_3$ and $t_{23}=0$. In case of an inhomogeneously broadened transition, the two-pulse signal is also emitted time delayed as a spontaneous photon echo.[55]

After the first demonstration of photon echo pulses from ruby crystals,[56,57] the photon echo technique was also used to study bound exciton states both in II-VI semiconductors[58] and III-V semiconductors.[59,60] In recent years, dephasing studies on intrinsic excitations in semiconductors have attracted increasing interest.[61] Here we briefly summarize dephasing results obtained for optical excitations in the ordered semiconductors GaAs and CdSe in order to point out the characteristic changes in the dephasing behavior introduced by disorder and localization.

A very short dephasing time of several tens of femtoseconds has been reported for free-electron–hole pairs in GaAs at high carrier densities well above 10^{17} cm^{-3} and excitation with considerable excess energy.[62] Dephasing is dominated by carrier-carrier scattering under these experimental conditions. In contrast, phase relaxation of free excitons in GaAs is much slower with typical dephasing times of several picoseconds. Depending on exciton density and temperature, exciton-exciton or exciton-phonon scattering are the mechanisms mainly contributing to dephasing in this situation.[24,25]

Dephasing of quasi-two-dimensional excitons in $GaAs/Al_xGa_{1-x}As$ quantum wells has also been studied intensively. The dephasing times of predominantly homogeneously broadened excitons in quantum wells[63] are comparable to the dephasing times of three-dimensional excitons. The dephasing times of excitons are slightly longer in quantum wells which show inhomogeneous broadening due to interface roughness,[64–67] indicating that disorder may also modify the dynamics of excitons in two-dimensional systems.

Phase relaxation of free excitons in CdSe has been studied in Refs. 22 and 23. Dephasing times of up to 40 ps at 4.2 K and low excitation intensities have been reported, which is slightly longer than in GaAs. The dephasing is governed by exciton-exciton and exciton-phonon scattering very similar to GaAs. Consequently, an increase of exciton density or temperature results in a considerable decrease of the dephasing times.

IV. THEORETICAL BASIS

A. General outline

Our theoretical treatment of the photon echo in disordered semiconductors is based on a perturbative solution (with respect to the external laser field) of the optical Bloch equations.[68,69] We include static disorder, electron-phonon coupling, and electron-hole Coulomb interaction. Many-body effects such as electron-electron and hole-hole interaction as well as electron-hole contributions beyond the electron-hole attraction are neglected.[10–12] In perfect crystalline semiconductors these terms lead to dramatic effects,[70–72] which have also been seen experimentally.[73,70] In a disordered semiconductor, however, many-body effects are less important due to the inherent inhomogeneity of these systems. Therefore, we restrict our model to the direct electron-hole attraction. We note, however, that a more complete theory is needed to clarify this point.

We choose a tight-binding model system with site-diagonal electron-phonon coupling in order to interpret the general trends seen in the experimental data and to clarify the underlying microscopic processes leading to optical dephasing. We then employ the small-polaron transformation, which leads to a dynamical renormalization of the intersite transfer-matrix elements and of the intrasite polarization.

The amplitude of the spontaneous photon echo is calculated at the time of its maximum $t=2t_{21}$. It is propor-

tional to the third-order optical polarization $P^{(3)}(t)$ at this time, averaged over the thermal phonon ensemble and the configuration of the static disorder potential. The observed photon echo amplitude is then proportional to

$$P^{(3)}(2t_{21}) \propto \langle\langle\{\Delta_{\mathbf{k}}(2t_{21})|U(2t_{21},t_{21}) \times \Delta_{\mathbf{k}_2}(t_{21})[U(t_{21},0)\Delta_{\mathbf{k}_1}(0)]^{+} \times \Delta_{\mathbf{k}_2}(t_{21})\}\rangle_{\mathrm{ph}}\rangle_{\mathrm{conf}}, \quad (3)$$

where we use the tensor notation of Ref. 12 in the space spanned by the site functions. The excitation pulses have been assumed to be of $\delta(t)$ form, i.e., shorter than all relevant time scales in the system. Expression (3) has a direct physical interpretation: at time $t=0$ the first very short laser pulse arrives at the sample and excites all sites, described by the polarization vector $\Delta_{\mathbf{k}_1}(0)$. For later times, the resulting polarization develops according to the evolution operator $U(t,0)$, containing disorder, Coulomb interaction, and phonon coupling. At time $t=t_{21}$, the second laser pulse arrives $[\Delta_{\mathbf{k}_2}(t_{21})]$ and interacts nonlinearly with the polarization pattern present at that time, $U(t_{21},0)\Delta_{\mathbf{k}_1}(0)$, producing the conjugated pattern $[U(t_{21},0)\Delta_{\mathbf{k}_1}(0)]^{+}$ and the population pattern $[U(t_{21},0)\Delta_{\mathbf{k}_1}(0)]^{+}\Delta_{\mathbf{k}_2}(t_{21})$. The same pulse interacts with this population pattern resulting in a polarization $\Delta_{\mathbf{k}_2}(t_{21})[U(t_{21},0)\Delta_{\mathbf{k}_1}(0)]^{+}\Delta_{\mathbf{k}_2}(t_{21})$, which freely evolves in time according to $U(t,t_{21})$. At time $t=2t_{21}$, the resulting polarization pattern is compared with the macroscopic polarization $\Delta_{\mathbf{k}}(2t_{21})$, which leads to the echo signal at $t=2t_{21}$ in the direction $\mathbf{k}$. This overlap determines the strength of the echo signal.

Alternatively, expression (3) can also be viewed as a correlation function, which describes the correlation of polarization amplitude dynamics in one time interval $(0,t_{21})$ with that in the second interval $(2t_{21},t_{21})$. In the absence of phonons, the correlation of the propagation in the actually different time intervals can also be expressed as a correlation of propagation in the intervals $(0,t_{21})$ and $(t_{21},0)$. It is interesting to note that this type of correlation is at the heart of Anderson localization.[74] In fact, it can be shown that, in contrast to linear optics, nonlinear optical experiments are in principle capable of showing critical behavior due to Anderson localization.[10,11]

We proceed by presenting a discussion of the results for a number of model cases, without going into the details of the derivation which can be found elsewhere.[10–12,75] As a first step, we exclude Coulomb interaction and phonons in order to show the influence of static disorder alone on the decay of the photon echo amplitude. Two cases are of particular interest: a strongly disordered semiconductor and a nearly perfect crystalline semiconductor with weak disorder. In the first case, all or nearly all states are localized, with a localization radius depending on the ratio of disorder and intersite transfer. In the second case, the states are delocalized except at the band extremities. The appropriate physical picture is that of scattering of free electrons and holes at the disorder potential. Next we include electron-hole attraction and consider different types of excitonic excitations. Finally we add the electron-phonon coupling and discuss in particular the case of excitons bound to short-range valence-band edge fluctuations. This model will lead to a satisfactory interpretation of the data on the temperature dependence of the dephasing rate reported in Sec. V.

B. The influence of disorder on the dephasing rate

Our tight-binding model is determined by three parameters $\eta_v = W_v/J_v$, $\eta_c = W_c/J_c$, and the length scale of the disorder potential, where W_c, W_v are the widths of the diagonal disorder distributions and J_c, J_v are the nearest-neighbor transfer elements of the electron and hole states at the individual sites, respectively. We recall that a perfectly ordered band with Bloch states is described by $\eta=0$ while strongly localized states in a disordered band are characterized by $\eta=\infty$. In all cases treated below, carrier-carrier scattering is excluded. The following results are obtained within the model.

1. $\eta_v=\infty$, strongly localized holes, Coulomb interaction excluded, no phonons

There is no dephasing if $\eta_c=\infty$ (uncoupled inhomogeneously distributed two-level absorbers). An initial fast decay of the photon echo amplitude followed by a constant long-time value, proportional to the inverse square of the localization length of electrons, is found for $\eta_c<\infty$. The long-time value of the polarization $P^{(3)}(2t_{21})$ is finite if η_c is larger than the critical value where Anderson localization disappears. For η_c smaller than the critical value, the echo decays towards zero on a time scale determined by the inverse of the electron bandwidth or of the spectral laser width, whichever is smaller. Consequently, mutually uncoupled strongly localized holes ($\eta_v=\infty$) and Bloch electrons ($\eta_c=0$) produce an extremely fast decay of the polarization $P^{(3)}(2t_{21})$.

2. $\eta_c=0$, Coulomb interaction excluded, no phonons

For a perfect crystalline semiconductor ($\eta_v=0,\eta_c=0$), we again have a nondecaying echo signal due to the inhomogeneous nature of the optical band-band transitions, which form an ensemble of uncoupled two-level absorbers in $\mathbf{k}$ space. If disorder is introduced, e.g., in the valence band ($\eta_v>0$), dephasing occurs due to scattering, i.e., due to disorder-induced coupling of different $\mathbf{k}$ states. We note, however, that this model is rather academic since Coulomb interaction cannot be neglected for near-band-gap transitions in an ordered or only slightly disordered semiconductor.

3. Excitons, strongly localized holes, $\eta_v=\infty$, no phonons

We assume that the holes are strongly localized in a disordered valence band. As Coulomb attraction is now included in the model, the electrons are bound to the holes and immobile, strongly localized excitons are

formed. Note that, within this model, exciton localization results from the localization of the hole. Since the excitons are immobile, the energy spectrum of each local exciton is in part discrete. Disorder results in an inhomogeneous distribution of these local, partly discrete spectra of the excitons. Depending on the spectral width of the laser pulses, one or more discrete energy levels of each local spectrum are excited. First, we consider the extreme case of $\delta(t)$-like excitation pulses with a white pulse spectrum. In this case, we find a beating polarization for one local exciton according to

$$P^{(3)}(2t_{21}) \propto \left| \sum_n |\Psi_n(\mathbf{r}=0)|^2 \exp(i\varepsilon_n t_{21}) \right|^2 . \quad (4)$$

Here $\Psi_n(\mathbf{r})$ and ε_n denote the wave functions and the eigenenergies of the eigenstates of a local exciton, respectively. Equation (4) resembles the case of quantum beats in an N-level system, where the resonances with energy ε_n have matrix elements proportional to $|\Psi_n(\mathbf{r}=0)|^2$. Excitation pulses with a broad pulse spectrum excite a variety of energy levels of each exciton. As a result of the inhomogeneous distribution of energy spectra, the superposition of beating signals produces an initial fast decay of the echo amplitude on the time scale of the pulse duration followed by a constant long-time value. The magnitude of the long-time value depends on the relative strengths of the optical transitions with energy ε_n.

In the case of an ordered conduction band ($\eta_c = 0$), the wave functions are hydrogenic and the terms $|\Psi_n(\mathbf{r}=0)|^2$ decrease with increasing n according to $|\Psi_n(\mathbf{r}=0)|^2 \propto n^{-3}$. The first term in the sum of Eq. (4) then dominates at long times, leading to a finite value of the echo amplitude in the long-time limit. Thus, we do not find optical dephasing due to disorder in this particular case. This result is in contrast to the finding obtained for the model which excludes Coulomb interaction and shows that Coulomb interaction has a stabilizing effect on the optical phase.

The same argument as in the case of the ordered conduction band applies if the disorder potential seen by the electron fluctuates on a length scale larger than the exciton Bohr radius. In this case, the potential is nearly constant over the Bohr radius and there is no dephasing due to disorder.

In contrast, a disorder potential varying on a length scale comparable to the Bohr radius mixes the excitonic eigenstates, which are then no longer hydrogenic. The various terms in the sum of Eq. (4) will be of comparable magnitude resulting in a larger modulation of the beating signal of one localized exciton. The inhomogeneous distribution then leads to an initially decaying signal with a long-time value which is smaller than that of the pure hydrogenic exciton. In other words, short-range disorder leads to dephasing of strongly localized excitons if the laser pulse spectrum is sufficiently broad.

Finally, we mention the situation where the system is excited by spectrally narrow laser pulses, which excite only the lowest level of each exciton energy spectrum. This case is analogous to the ensemble of uncoupled two-level absorbers discussed above and there is no disorder-induced dephasing for any kind of disorder.

4. Mobile excitons, no phonons

In this subsection, the term "mobile exciton" applies to both delocalized excitons and to excitons localized as a whole with a localization radius larger than the exciton Bohr radius. As a result of disorder, mobile excitons are characterized by an optical spectrum which does not consist of discrete excitation levels since the excitonic eigenstates cannot be classified by the vector $\mathbf{K}$ of the center-of-mass momentum. In other words, $\mathbf{K}$ is not a good quantum number in a disordered semiconductor. However, the optical excitation coherently drives a polarization with momentum $\mathbf{K}$ close to zero. Thus, a noneigenstate is prepared by the excitation laser pulse and consequently a complicated temporal evolution of the excited wave function follows the excitation. This evolution involves scattering of the center-of-mass momentum since $\mathbf{K}$ is not conserved. In addition, mixing of the hydrogenic states describing the relative motion between electron and hole occurs if the potential contains fluctuations which are short range compared to the exciton Bohr radius. A decay of the optical phase is then to be expected on a time scale given roughly by the laser pulse width.

However, there is a particular case where (essentially) no dephasing exists.[12] Consider a disorder potential which only acts on the center-of-mass coordinate, i.e., a disorder potential which is long range compared to the exciton Bohr radius. Then the initially excited polarization pattern is distorted in the course of time due to scattering of the center-of-mass momentum $\mathbf{K}$. However, nonlinear interaction with the second excitation pulse at time $t = t_{21}$ produces a polarization pattern which is phase conjugated to the distorted one. The phase-conjugated pattern then (nearly) perfectly evolves back in time producing the initial plane wave at the time $t = 2t_{21}$, albeit in the kinematic direction $2\mathbf{k}_2 - \mathbf{k}_1$. Short-range disorder acting on the relative motion disturbs the perfect phase conjugation and consequently leads to initial or even total dephasing on a short time scale as discussed above.

C. Phonon contributions to the dephasing rate

We now turn to the discussion of the influence of the electron-phonon coupling in these model cases. We first recall that the small-polaron transformation renormalizes both the interband polarization operators $\Delta_{\mathbf{k}_1}(t), \Delta_{\mathbf{k}_2}(t)$ and the intraband dynamics given by the transfer terms J_c, J_v. All these operators now contain phonon degrees of freedom. The first group of interband polarization operators describes the phonon contributions to the intrasite optical line shapes[76] while the second group of transfer terms describes phonon-assisted hopping and phonon-induced delocalization.[3–5,75] It is a plausible approximation to assume that both processes are uncorrelated. Furthermore, the intrasite dephasing takes place on a short time scale, comparable to phonon frequencies, and in general leaves us with a finite long-time value of the signal. We then write the intensity as a product

$$I(2t_{21}) \propto |\langle\langle[\Delta_{\mathbf{k}}(2t_{21})|\Delta_{\mathbf{k}_2}(t_{21})\Delta_{\mathbf{k}_1}(0)^{+}\Delta_{\mathbf{k}_2}(t_{21})]\rangle_{\mathrm{ph}}\rangle_{\mathrm{conf}}\langle\langle\{\mathbf{1}|U(2t_{21},t_{21})\mathbf{1}[U(t_{21},0)\mathbf{1}]^{+}\mathbf{1}\}\rangle_{\mathrm{ph}}\rangle_{\mathrm{conf}}|^2 . \quad (5)$$

The first factor is a (fourth order with respect to the polarization operators) line-shape function in the time domain. The analogous second-order line-shape function in the frequency domain has been studied extensively by Duke and Mahan.[77] The second factor contains information about dephasing due to intersite dynamics such as, e.g., hopping.

Let us first concentrate on the first factor. It can be evaluated following the lines of Duke and Mahan for various models of the electron-phonon coupling (e.g., acoustic deformation potential and screened piezoelectric interaction). There are three contributions to the line shape and thus to dephasing: spontaneous phonon emission, stimulated phonon emission, and phonon absorption. In addition, there is a constant term if the line has a $\delta(\omega)$-like zero-phonon contribution. It turns out that dephasing due to phonon absorption and stimulated emission is negligible at the low temperatures considered here (5–15 K). In this temperature range, spontaneous emission is the dominant process and leads to an initial fast decay on the time scale of an inverse typical phonon frequency. This time scale is of the order of one picosecond. The corresponding decay rate is independent of temperature. The fast decay is followed by a finite long-time value, which depends weakly on temperature. The small temperature-dependent dephasing rates seen in the experiments (see Sec. V) at longer times must therefore be due to intersite processes contained in the second factor of Eq. (5).

We now study the decay of the photon echo on a time scale longer than a phonon period (about 1 ps) and thus concentrate on the second factor. We specify the theoretical model for the particular case of $CdS_{1-x}Se_x$ mixed crystals. The model assumes that the hole is strongly localized in a disordered valence band whereas the electron is free in an ordered conduction band. Localization of the exciton is thus a result of Coulomb attraction between electron and hole. Due to the particular electronic band structure of $CdS_{1-x}Se_x$, this model is appropriate to describe exciton localization in $CdS_{1-x}Se_x$: In $CdS_{1-x}Se_x$ the valence-band states are mainly formed by the anions, whereas the conduction-band states originate from the cadmium cations (see Sec. II). According to this electronic structure it is evident that disorder mainly affects the valence band since disorder is present in the anion sublattice. The conduction band is nearly ordered.

As discussed previously, within this model a finite long-time value of the echo signal is obtained if phonon coupling is excluded. Our model for the slow dephasing at long times is the following. The coupling to the phonons allows the localized holes to hop between the relative maxima of the valence-band edge, i.e., between the localized valence-band tail states. The electron, being bound to the hole, follows this movement. However, any hopping event is an incoherent process, which irreversibly destroys the optical phase. We therefore identify the dephasing rate in the long-time limit with the hopping rates of holes.

The first hop of an exciton after generation leads to dephasing. In order to calculate the dephasing rate T_2^{-1} at excitation energy E_{exc}, one has to calculate the typical hopping rate of a hole at the initial localization energy $\varepsilon_{\mathrm{exc}}=E_b-E_{\mathrm{exc}}$ in the valence-band tail. Here E_b is the energy of the effective exciton mobility edge.

The hopping rate of localized holes depends on the energetic distribution of the localized valence-band tail states, the temperature, and the localization length α of the holes. In our model of localized holes, the localization length α of the holes is smaller than the Bohr radius. As discussed in Sec. II, an exponential form of the density-of-states distribution is usually assumed. The quantitative calculation in this section allows us to determine the particular form of the valence-band tail which leads to a reasonable agreement with the experimental data. The hopping rates of holes depend on the energetic position in the valence-band tail. Thus, in the experiments presented in Sec. V additional information is obtained by changing the excitation photon energy.

In our model, localization energies ε of holes in the valence-band tail are calculated with respect to the valence-band mobility edge, taken to be the zero point of the localization energy scale. After resonant excitation of an exciton with hole at an energy $\varepsilon_{\mathrm{exc}}$, the hole can hop down in energy to some deeper-lying localized state with localization energy $\varepsilon>\varepsilon_{\mathrm{exc}}$. This process is accompanied by emission of phonons and its typical rate $\nu_{\downarrow}(\varepsilon_{\mathrm{exc}})$ is

$$\nu_{\downarrow}(\varepsilon_{\mathrm{exc}})=\nu_0\exp[-2R(\varepsilon_{\mathrm{exc}})/\alpha] , \quad (6)$$

where $R(\varepsilon_{\mathrm{exc}})$ is the typical distance between localized states with localization energies larger than $\varepsilon_{\mathrm{exc}}$, and ν_0 is an attempt-to-escape frequency containing details of the hole-phonon coupling (in general, the attempt-to-escape frequency ν_0 depends on localization energy). If $g(\varepsilon)$ is the density of states in the valence-band tail, then

$$R(\varepsilon)=\left[(4\pi/3)\int_{\varepsilon}^{\infty} g(\tilde{\varepsilon})d\tilde{\varepsilon}\right]^{-1/3} . \quad (7)$$

At finite temperatures, a hole at localization energy $\varepsilon_{\mathrm{exc}}$ can also hop to some localized state at energy $\varepsilon<\varepsilon_{\mathrm{exc}}$ by absorbing phonons. The typical rate of this process is

$$\nu_{\uparrow}(\varepsilon_{\mathrm{exc}},\varepsilon)=\nu_0\exp[-2R(\varepsilon)/\alpha-(\varepsilon_{\mathrm{exc}}-\varepsilon)/kT] . \quad (8)$$

It is essential for our analysis to keep track of the correlation between hopping distances $R(\varepsilon)$ and the localization energy ε. In Eqs. (6) and (8) we have assumed that the tunneling of holes is the dominant process for exciton hopping in our system. The justification for this model partly comes from its success in describing time-resolved luminescence spectra in $CdS_{1-x}Se_x$.[7] On the other hand, dipole-dipole exciton transfer rates[78] can be considered. Dipole-dipole transfer rates are proportional to $R(\varepsilon)^{-6}$.

However, the following analysis does not yield the observed strong temperature dependence of the hopping rates for any reasonable density-of-states model if dipole-dipole interaction is assumed for the hopping process. We therefore conclude that in the energy and time regime of the present experiment, the hole tunneling rates are dominant as compared to the dipole-dipole transfer rates.

In order to fit the experimental data on the optical dephasing rate, we are interested in the typical fastest hop of a hole at an initial localization energy ε_{exc} and at a given temperature. The problem of typical hopping rates of carriers at finite temperatures was considered in Ref. 79 for an exponential density of states

$$g(\varepsilon)=(N_0/\varepsilon_0)\exp(-\varepsilon/\varepsilon_0) , \tag{9}$$

where N_0 is the total density of tail states and ε_0 is the energy scale of the tail. In this problem, the so-called transport energy[79] ε_T plays an important role:

$$\varepsilon_T=3\varepsilon_0\ln\left[\frac{3\varepsilon_0(N_0\alpha^3)^{1/3}}{2kT}\right] . \tag{10}$$

For states with $\varepsilon<\varepsilon_T$, the typical hopping rate is equal to $\nu_\downarrow(\varepsilon)$ [Eq. (6)] and for $\varepsilon>\varepsilon_T$ the rate of the fastest hop is equal to $\nu_\uparrow(\varepsilon,\varepsilon_T)$ [Eq. (8)]. In other words, for deeply localized states with $\varepsilon>\varepsilon_T$, the typical fastest hop is that to some state with energy ε_1 in the vicinity of the transport energy ε_T. This process is thermally activated. A pronounced temperature dependence can be expected in this case. On the other hand, for shallow states with $\varepsilon<\varepsilon_T$, the temperature-independent hops downward in energy dominate the hopping of carriers.

Here we extend this approach for the calculation of typical hopping rates to a rather wide class of functions $g(\varepsilon)$. Our aim is to find the appropriate shape of the valence-band tail which fits the experimental data on the optical dephasing of excitons, in particular the temperature dependence of the dephasing rates.

Different shapes of the density of tail states were suggested in the past for mixed crystals on the basis of different theoretical and experimental studies.[34,35,80,37] We note that almost all of them have the form

$$g(\varepsilon)=(N_0/\varepsilon_0)C(\beta)\exp[-(\varepsilon/\varepsilon_0)^\beta] , \tag{11}$$

where the exponent β is in the range 0.5–2 and $C(\beta)$ is a normalization factor.

We use the following algorithm for calculating the rate of the typical fastest hop of a hole, which has been excited with an initial localization energy ε_{exc}. First, we take some particular shape of the density of states $g(\varepsilon)$. Then using Eqs. (6) and (7) we calculate the typical rate $\nu_\downarrow(\varepsilon_{exc})$ of a downward hop of a hole which has been prepared at the localization energy ε_{exc}. We also calculate the maximum hopping rate upwards in energy using Eqs. (7) and (8), sweeping the energy ε of the final state of the hop from ε_{exc} to the mobility edge ($\varepsilon=0$). If at some energy ε_t ($0<\varepsilon_t<\varepsilon_{exc}$) a maximum hopping rate $\nu_{max}(\varepsilon_{exc},\varepsilon_t)$ exists, we compare ε_t to ε_{exc}. In some cases we find that $\varepsilon_t=\varepsilon_{exc}$, indicating that the typical fastest hop occurs downwards in energy towards deeper-lying localized states. If we find that $\varepsilon_t<\varepsilon_{exc}$, then $\nu_\uparrow(\varepsilon_{exc},\varepsilon_t)>\nu_\downarrow(\varepsilon_{exc})$ because of the monotonously decreasing density-of-states function. Consequently, the typical fastest hop is then provided by thermal activation of a hole due to absorption of phonons. The energy ε_t which provides the fastest activation of holes is the analog to the transport energy of Ref. 79. In all cases, the optical dephasing rate is identified with the maximum hopping rate determined by the procedure described above.

The parameters of this model are (i) the exponent β, which will be determined from a fit to the temperature dependence of the dephasing rate at the lower excitation energy, (ii) N_0 and ε_0, which are at least approximately known from luminescence experiments, (iii) the localization radius α, which is usually taken to be related to N_0 by $N_0\alpha^3\simeq 1$, and finally (iv) ν_0, which can be obtained from a fit to the dephasing rate at low temperatures. We know from conventional hopping theories[81] that for single-phonon processes the electron- (hole-) phonon interaction rate increases with decreasing localization radius α. Hence ν_0 increases with increasing localization energy, i.e., with decreasing excitation energy.

V. EXPERIMENTAL RESULTS: $CdS_{1-x}Se_x$

The FWM and photon echo experiments have been performed on high-quality platelets of $CdS_{1-x}Se_x$ with thicknesses of 10–40 μm. The selenium content of the samples is either 38% or 60% corresponding to band-gap energies of 2.22 or 2.06 eV, respectively. Thus, the composition of the mixed-crystal samples is in the range where at low temperatures excitons are localized in the fluctuating disorder potential. The inhomogeneous width of the excitonic luminescence band amounts to 10 or 15 meV in our samples.

All of the experimental data presented in the following are obtained for resonant excitation of localized exciton transitions, i.e., for excitation photon energies within the excitonic photoluminescence band. These excitation photon energies also correspond to the tail of the absorption spectrum. The excitation field is perpendicularly polarized to the optical axis of the crystals. Thus, we have studied transitions involving the upper valence band. All data are obtained at low temperatures between 1.8 and 15 K to avoid thermal delocalization of excitons.

The samples are excited by pulses from a synchronously mode-locked dye laser with pulse durations of 7–10 ps and a spectral width of less than 0.5 meV. This experimental setup allows both temporal and spectral resolution with sufficient accuracy. In particular, using a narrow pulse spectrum we avoid additional excitation of delocalized excitons which is reported for experiments on $CdS_{1-x}Se_x$ with pulses of 5-ps duration or less.[82] According to Ref. 82, delocalized excitons can be excited by the high-energy part of a broad pulse spectrum even if the center part of the pulse spectrum is resonant to localized exciton transitions. The implications of simultaneous generation of delocalized excitons on the dephasing of localized excitons are also discussed in Ref. 82.

The FWM signals are recorded either time integrated with a slow photodetector or in real time with a syn-

chroscan streak camera providing a time resolution of 15 ps.

The result of a time-resolved spontaneous photon echo experiment on a $CdS_{1-x}Se_x$ mixed crystal with 60% selenium is shown in Fig. 2. Original streak camera traces are depicted for different time delays t_{21} between pulse no. 1 and pulse no. 2. From the bottom to the top the time delay t_{21} increases from 70 to 160 ps. The intensity of the excitation pulses after passing through the sample is arbitrarily attenuated and therefore not to scale. It only serves to mark the temporal position of the excitation pulses. These data clearly show the emission of the spontaneous photon echo (shaded pulse) even at time delays t_{21} as large as 160 ps. Consequently, the dephasing time of resonantly excited localized excitons in $CdS_{1-x}Se_x$ mixed crystals has to be long compared to the dephasing times of free excitons in the corresponding binary compound CdSe, where disorder and localization are absent. In fact, we find a dephasing time of 340 ps for localized excitons in the mixed crystal under these experimental conditions (temperature 10 K, exciton density about 10^{16} cm^{-3}). This dephasing time is longer by about one order of magnitude than the dephasing time of free excitons in CdSe, which amounts to less than 40 ps.[22,23]

We have also demonstrated the emission of stimulated photon echo pulses from localized exciton transitions in $CdS_{1-x}Se_x$ mixed crystals. Streak camera traces showing the result of a three-pulse FWM experiment are depicted in Fig. 3. The time delay t_{21} between pulse no. 1 and pulse no. 2 varies from -40 ps (bottom) to $+130$ ps (top). As in the preceding figure, the amplitudes of the incoming excitation pulses are arbitrary in this figure and only mark the temporal position of the respective pulses. For negative time delays t_{21}, i.e., if pulse no. 2 precedes pulse no. 1, no echo pulse is emitted in the phase-matching direction $\mathbf{k}_4=\mathbf{k}_3+\mathbf{k}_2-\mathbf{k}_1$ of the camera. However, at positive time separations, the time-delayed emission of stimulated photon echo pulses is clearly demonstrated. The dephasing time obtained from the stimulated photon echo decay is equal to the dephasing time constant evaluated from spontaneous photon echo experiments. In addition, we note that the observation of a photon echo unambiguously demonstrates the inhomogeneous broadening of localized exciton transitions in $CdS_{1-x}Se_x$.

We have also investigated $CdS_{1-x}Se_x$ mixed crystals with 38% selenium instead of 60%. The main features of the FWM experiments discussed so far are also found for $CdS_{0.62}Se_{0.38}$ samples: (i) the inhomogeneous nature of localized exciton transitions giving rise to photon echo emission, and (ii) the long dephasing times of several hundreds of picoseconds.

Comparing the long dephasing times of localized excitons in $CdS_{1-x}Se_x$ mixed crystals to the short dephasing times of free excitons in ordered CdSe,[22,23] we consequently conclude that in $CdS_{1-x}Se_x$ mixed crystals localization strongly reduces exciton-exciton and exciton-phonon scattering. The dynamics of localized excitons are comparable to the findings for impurity-bound excitons in CdS and CdSe, which also show long dephasing times.[83,84]

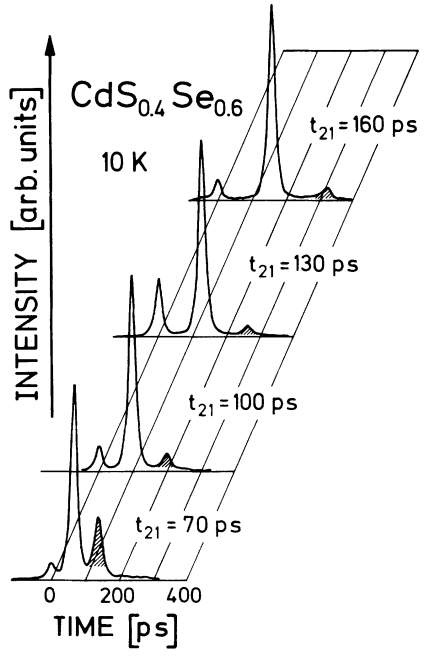

FIG. 2. Time-resolved streak camera traces showing the emission of spontaneous photon echo pulses (shaded) from a $CdS_{1-x}Se_x$ mixed crystal for resonant excitation of localized excitons. The time delay t_{21} between the excitation pulses increases from the bottom to the top. The intensity of the excitation pulses is arbitrarily attenuated in each pulse sequence. The dephasing time amounts to 340 ps at a temperature of 10 K.

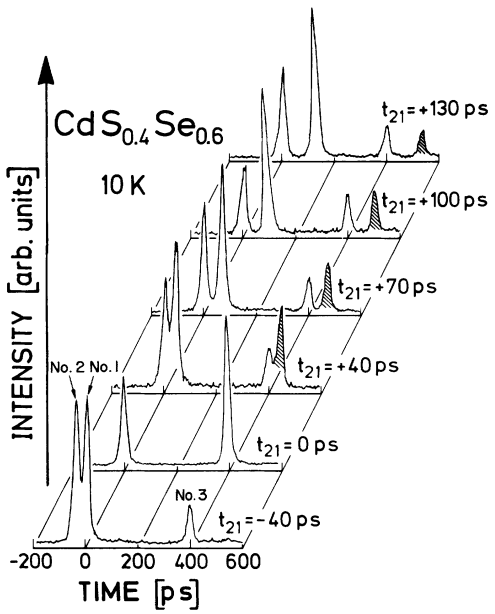

FIG. 3. Streak camera traces of stimulated photon echo pulses (shaded) from localized exciton transitions in $CdS_{1-x}Se_x$. The sample temperature amounts to 10 K. The time delay t_{21} between excitation pulse no. 1 and excitation pulse no. 2 increases from the bottom to the top; the intensity of the excitation pulses is not to scale.

In the following, we will present and discuss the results for the intensity, energy, and temperature dependence of the dephasing time of localized excitons. The different contributions to the total dephasing rate can be separated and the main mechanism for dephasing can be identified. The disorder-induced contribution to dephasing can also be determined.

We have determined the dephasing time of localized excitons in dependence of exciton density in order to study the contribution of exciton-exciton scattering to dephasing. Figure 4 shows in a semilogarithmic plot the time-integrated stimulated photon echo intensity as a function of time delay t_{21} for different excitation intensities. The maximum intensity corresponds to an exciton density of 10^{16} cm^{-3}. The data are obtained for a sample with 60% selenium at a temperature of 10 K. For clarity of the presentation, the curves are arbitrarily shifted along the vertical axis. All the curves show a nonexponential decay with a fast decay at early times, which is not resolved by the 7-ps pulses applied in this experiment. The fast decay is followed by a slower component at longer time delays. The slowly decaying part of the signal reflects the long-time dephasing of resonantly excited localized excitons, which has also been observed in the time-resolved photon echo experiments. The rapidly decaying contribution is assigned to the phonon-induced intrasite dephasing process discussed in Sec. IV. It should be mentioned at this point that a relative increase of the fast component is reported in Ref. 82 for excitation by shorter pulses with an accordingly broader spectrum. Under these experimental conditions, the fast component partly results from dephasing of delocalized excitons, which are excited in addition to localized ones.[82]

With respect to the present discussion, however, the main feature of the data presented in Fig. 4 is that the long-time behavior of the dephasing signal is independent of the excitation intensity. Consequently, the dephasing time of localized excitons does not depend on exciton density in the density range we have investigated, i.e., up to densities of 10^{16} cm^{-3}. Interaction between localized excitons is thus negligible in this density range. This experimental finding is in contrast to the experimental results obtained for free excitons in the ordered binary compound semiconductor CdSe,[22,23] where exciton-exciton scattering is an efficient scattering mechanism, which leads to a decrease of the dephasing time with increasing exciton density. This comparison demonstrates the considerable impact of localization on exciton dynamics in $CdS_{1-x}Se_x$ mixed crystals.

As exciton-exciton scattering does not contribute to dephasing in the density range under consideration, the observed dephasing rates can only result from the population decay, i.e., energy relaxation (exciton-phonon interaction) and recombination, and from disorder scattering.

We have measured the dephasing time in dependence of excitation photon energy in order to gain further insight into the microscopic mechanism of dephasing. Results are shown in Fig. 5, where the dephasing time is plotted as a function of excitation energy. The data are obtained at a temperature of 10 K using a sample with 60% selenium. The inset shows the photoluminescence spectrum of the sample for above-band-gap excitation in order to illustrate the energy range where the data have been taken. The spectrum is dominated by the excitonic luminescence band with an inhomogeneous width of about 10 meV. Phonon replicas are also resolved at lower energies. The shaded region corresponds to the energy range where the dephasing experiments have been performed. In this region, the measured dephasing times

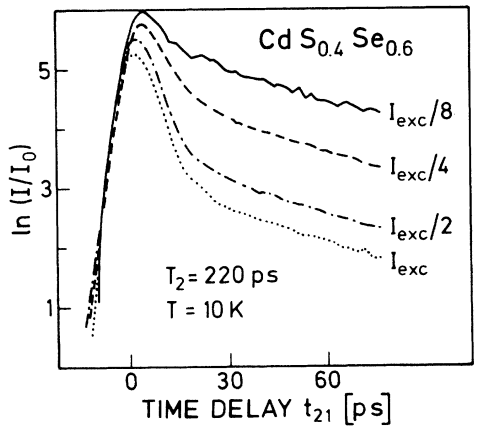

FIG. 4. Semilogarithmic plot of the time-integrated stimulated photon echo intensity from localized exciton transitions in $CdS_{1-x}Se_x$ as a function of time delay t_{21}. The excitation intensity increases from the solid-line curve to the dashed one and further to the dashed-dotted and the dotted one. The maximum intensity corresponds to an exciton density of 10^{16} cm^{-3}. The data are obtained at a temperature of 10 K and a dephasing time of 220 ps is inferred from the results. The curves are arbitrarily shifted along the vertical axis.

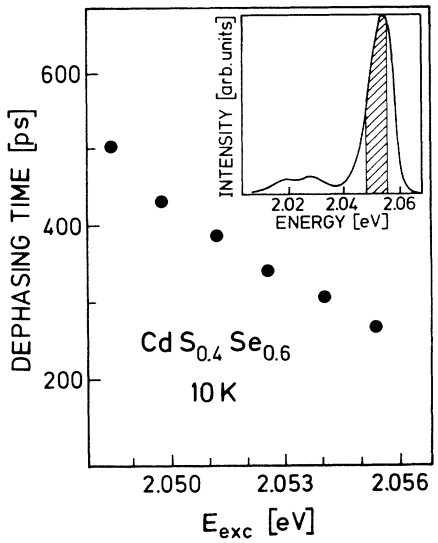

FIG. 5. Dephasing time of localized excitons in $CdS_{1-x}Se_x$ mixed crystals as a function of excitation photon energy at a temperature of 10 K. The inset shows the photoluminescence spectrum of the sample, in which the shaded region corresponds to the spectral range where the dephasing times have been determined.

increase from 260 ps at the high-energy side to 500 ps at the low-energy side. The excitation intensity has been kept constant in the experiment, yet in the entire regime the dephasing times do not depend on excitation density for exciton densities below 10^{16} cm^{-3}. Thus, we can definitely rule out that the decrease of the dephasing time with increasing excitation photon energy results from the onset of exciton-exciton scattering. In the following, we show that the observed energy dependence of the dephasing time is related to disorder.

We find qualitatively the same energy dependence of the dephasing time for samples with a selenium content of 38%. In addition, the same energy dependence of the dephasing time has been found at a temperature of 1.8 K instead of 10 K, yet with decreasing temperature we observe an increase of the dephasing time. For example, an increase of T_2 to 2 ns is found at $T=1.8$ K for an excitation photon energy corresponding to the low-energy side of the exciton photoluminescence band.

The same energy dependence as observed for the dephasing time is reported for the intraband energy relaxation time T_3 based on time-resolved photoluminescence studies.[7-9] In disordered semiconductors, the energy relaxation time T_3 describes phonon-assisted hopping processes within the distribution of the localized states. The dephasing time T_2, the energy relaxation time T_3, and the recombination time T_1 are connected by the fundamental relation

$$1/T_2 \geq 1/2T_3 + 1/2T_1 \ , \tag{12}$$

which originates from the fact that population decay is always accompanied by phase relaxation. If elastic scattering is absent, both sides of relation (12) are equal.

The dephasing times displayed in Fig. 5 are of the order of 100 ps while the recombination time is in the nanosecond range in $CdS_{1-x}Se_x$. Therefore, the recombination time can be neglected in terms of phase relaxation under these experimental conditions. Then the energy relaxation time T_3 sets an upper limit to the dephasing time according to $T_2 \leq 2T_3$. The dephasing times measured in our experiment are actually very close to the upper limit defined by the intraband energy relaxation times. These intraband energy relaxation times have been independently determined by photoluminescence.[7-9] Consequently, phase relaxation of localized excitons in $CdS_{1-x}Se_x$ is mainly due to energy relaxation, i.e., phonon-assisted hopping.

At excitation photon energies corresponding to the very-low-energy edge of the photoluminescence band and at the very low temperature of 1.8 K the hopping rates become so small that recombination can no longer be neglected. The dephasing time amounts to about 2 ns under these experimental conditions and is determined by both hopping and recombination. In order to generalize our main conclusion, we state that dephasing of localized excitons in $CdS_{1-x}Se_x$ results mainly from the population decay, including energy relaxation due to hopping and recombination. Hopping processes dominate the dephasing apart from the particular case where very deeply localized excitons are excited at temperatures well below 5 K. The observed energy dependence of the dephasing time thus reflects the energy dependence of the hopping rates. Disorder-induced dephasing obviously does not significantly contribute to the total dephasing rate.

Measurements of the dephasing rate as a function of temperature confirm these results. These experiments provide further support that hopping is the main dephasing mechanism. In addition, insight into the mechanism of localization is obtained from these data.

The dephasing rate is plotted as a function of temperature in the temperature range 5–15 K for two different excitation photon energies in Fig. 6. Circles mark the experimental data obtained at the lower excitation energy while squares correspond to the experimental data obtained at the higher excitation energy.

The main features of the experimental data are as follows: (i) The dephasing rate increases with temperature. This increase is more pronounced at the lower excitation energy while the temperature dependence at the higher excitation energy is only weak. At the higher excitation energy, the dependence of the dephasing rate on temperature is roughly linear. (ii) The dephasing rate at the higher excitation energy is larger than at the lower excitation energy at temperatures below 12 K. This relation is reversed at temperatures above 12 K. Thus a remarkable crossover is found.

These experimental results can quantitatively be described by the hopping model outlined in Sec. IV. The model assumes strong localization of holes. The dynamics of localized excitons involves tunneling-related hopping processes of holes.

The temperature dependence of the dephasing rate has been fitted quantitatively at the lower excitation energy of 2.208 eV. A localization energy of 15 meV has been used for the calculation since the mobility edge in the sample is at 2.223 eV. The density-of-states parameter ε_0 amounts to 5 meV in $CdS_{1-x}Se_x$ (Ref. 36) and the usual assumption on the localization radius α is made ($N_0\alpha^3=1$). With these input parameters an excellent fit to the experimental data is obtained (solid line in Fig. 6) by choosing the exponent β in Eq. (11) as 1.23 and by adjusting the attempt-to-escape frequency ν_0 at the low-temperature data point. A possible temperature dependence of ν_0 is usually weak and can thus be neglected compared to the strong temperature dependence of the exponential factor.

The higher excitation energy of 2.216 eV corresponds to shallow localized exciton transitions with a localization energy of 7 meV. At this energy, no temperature dependence of the dephasing time is obtained from our model calculation, which is based on the same input parameters as in the case of the deeply localized excitons, including the value $\beta=1.23$, which has been determined from the fit at the larger localization energy. The attempt-to-escape frequency ν_0 has been chosen to reproduce the low-temperature data point. The value of ν_0 at the lower localization energy (10^{12} s^{-1}) is smaller than the value obtained at the larger localization energy (4×10^{14} s^{-1}). As outlined in Sec. IV, this kind of energy dependence of ν_0 has to be expected and can be related to a slight change of the localization radius α by a factor

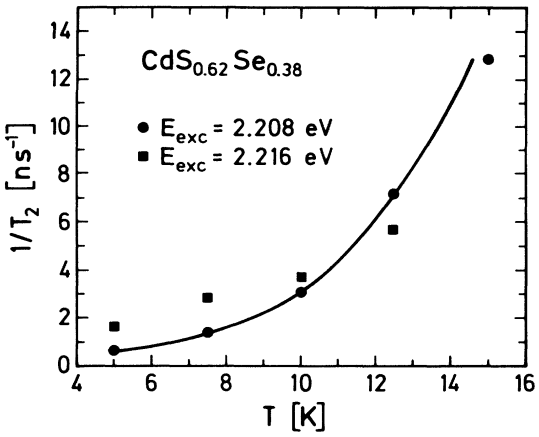

FIG. 6. Dephasing rate of localized excitons in $CdS_{1-x}Se_x$ mixed crystals as a function of temperature for two different excitation photon energies. Circles correspond to the lower excitation energy and squares to the higher excitation energy. The data obtained at the lower excitation photon energy have been fitted (solid line) with the hopping model discussed in Sec. IV.

less than 2.

It can easily be understood that the theory does not predict any temperature dependence of the dephasing rate at the lower localization energy (i.e., the higher excitation energy): in this case excitons are excited above the transport energy ε_T and thus temperature-independent hopping-down processes prevail against thermally activated hopping-up processes. The existence of the crossover is then a natural consequence of the fact that the exciton dynamics is dominated by thermally activated hopping-up processes at the larger localization energy while temperature-independent hopping-down processes (however with smaller prefactor ν_0) dominate at the lower localization energy.

The model reproduces the experimental finding that the temperature dependence of the dephasing rate is more or less pronounced, depending on localization energy. There is a slight discrepancy between the experimental data obtained at the higher excitation energy and the result of the model calculation. While the model predicts no temperature dependence of the dephasing rate, a slight, roughly linear increase of the dephasing rate with increasing temperature is observed experimentally. The dephasing rate increases by a factor 3 in the temperature range 5–15 K. This discrepancy shows that the temperature dependence of the attempt-to-escape frequency ν_0 cannot be neglected if the exponential factor does not depend on temperature. In fact, it is known that the phonon scattering rate of delocalized excitations linearly increases with temperature. It is reasonable to assume that this dependence is also valid for shallow localized excitons. This could account for the experimentally observed temperature dependence at the higher excitation energy.

In any case, based on the good agreement between the experimental findings and the model calculation, we conclude that in $CdS_{1-x}Se_x$ mixed crystals excitons are localized via the holes. We further conclude that dephasing of these localized excitons is mainly due to hopping processes related to phonon-assisted hole tunneling. Dipole-dipole transfer processes are negligible in $CdS_{1-x}Se_x$.

We now turn to the problem of disorder-induced phase relaxation. As mentioned above, the photon echo experiments show that disorder does not result in optical dephasing in $CdS_{1-x}Se_x$ mixed crystals. The influence of disorder on optical dephasing has been treated theoretically in Sec. IV. We apply the model for exciton localization which has been discussed above. The model assumes localization of an exciton by the hole; the conduction band is assumed to be ordered. Theory then predicts no dephasing due to disorder, again in good agreement with the experimental finding.

We conclude this section by stating that photon echo experiments can provide insight into the effect of disorder and localization on exciton dynamics. We have shown for $CdS_{1-x}Se_x$ that the dephasing times are of the order of several hundreds of picoseconds due to localization. The dephasing times are so long because localization reduces exciton-exciton and exciton-phonon scattering rates in the long-time limit as compared to free excitons. Hopping processes, i.e., intersite exciton-phonon interaction, dominate the dephasing behavior. Disorder does not contribute to dephasing. In addition, we have presented evidence that localization of excitons takes place via holes in $CdS_{1-x}Se_x$ mixed crystals and that hopping is due to phonon-assisted tunneling of holes.

VI. EXPERIMENTAL RESULTS: $Al_xGa_{1-x}As$

We have studied optical dephasing in direct-gap $Al_xGa_{1-x}As$ mixed crystals with aluminum concentrations between 30% and 38%. The samples have been grown on GaAs substrates either by molecular beam epitaxy (MBE) or metal-organic chemical-vapor deposition (MOCVD). The GaAs substrate has been removed by wet etching to allow for transmission experiment. The thickness of the samples is about 1.5 μm. The FWM experiments in $Al_xGa_{1-x}As$ have been carried out with a hybridly mode-locked dye laser as excitation source producing pulses of 1-ps (incoherent) width. If not mentioned otherwise, all experiments have been performed at a temperature of 10 K.

In the following, we present experimental data for the sample that has been investigated most comprehensively. Discussing only data from one sample ensures that all the experimental data can be compared with each other. The sample has an aluminum concentration of 38% and has been grown by MBE. Samples grown by MOCVD and samples with a lower content of aluminum have shown a very similar dephasing behavior. Thus, on the base of our experimental data, the results presented below are representative for $Al_xGa_{1-x}As$ mixed crystals.

The photoluminescence spectrum of the $Al_{0.38}Ga_{0.62}As$ sample is depicted in Fig. 7 (solid line). The spectrum is dominated by the excitonic emission band with an inhomogeneous width of 13 meV. Luminescence from carbon-acceptor-related transitions is also observed at lower energies. The inhomogeneous width of the exciton transition is comparable to typical inhomogeneous

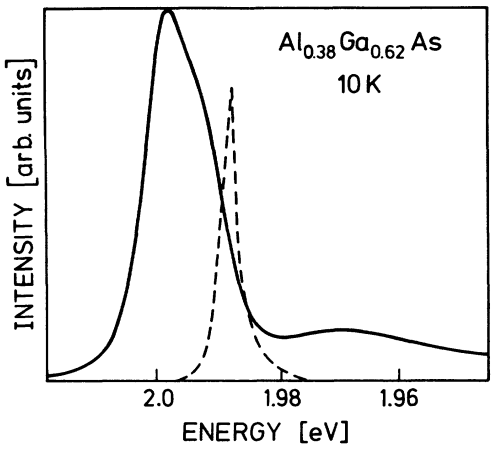

FIG. 7. Low-temperature photoluminescence spectrum (solid line) of the $Al_xGa_{1-x}As$ sample which has been studied by four-wave-mixing experiments. The dashed line shows the spectrum of the excitation pulses in order to characterize the spectral position of excitation.

linewidths of $CdS_{1-x}Se_x$ mixed crystals, indicating similar linear optical properties of both mixed-crystal systems in terms of disorder. The spectrum of the excitation pulse is also shown (dashed line) in Fig. 7 in order to characterize the excitation photon energy, where the FWM experiments have been performed. The excitation spectrum is centered at the low-energy side of the exciton luminescence band. The halfwidth of the pulse spectrum amounts to 3 meV, corresponding to a pulse coherence length of 0.7 ps, which also determines the time resolution in all experiments. The high-energy edge of the pulse spectrum coincides with the maximum of the exciton luminescence band. This choice of the excitation photon energy allows us to definitely rule out excitation of delocalized excitons or free-electron–hole pairs, despite of the broad pulse spectrum. Thus, scattering of excitons with delocalized excitations can be excluded. All the FWM signals discussed below are measured at the special position shown in Fig. 7.

The dephasing response of the $Al_xGa_{1-x}As$ sample is depicted in Fig. 8. In a semilogarithmic plot, the time-integrated spontaneous photon echo intensity is plotted as a function of time delay t_{21} for two different excitation densities N_0 and $N_0/2$. The curves are arbitrarily shifted along the vertical axis. The density N_0 amounts to 5×10^{14} cm^{-3}. At this density, a dephasing time of 5 ps is obtained from the experimental data. In addition, it is evident from the data depicted in Fig. 8 that the dephasing time does not increase if the exciton density is decreased from N_0 to $N_0/2$. As a consequence, exciton-exciton scattering should not significantly contribute to dephasing at these densities. Thus, the dephasing time of excitons in $Al_xGa_{1-x}As$ mixed crystals is considerably shorter than in $CdS_{1-x}Se_x$ and we can rule out that this finding is due to exciton-exciton interaction in $Al_xGa_{1-x}As$. The experimental result demonstrates that the nonlinear optical response of semiconductor mixed crystals sensitively depends on the detailed nature of the disorder, even in the case where the linear optical spectra

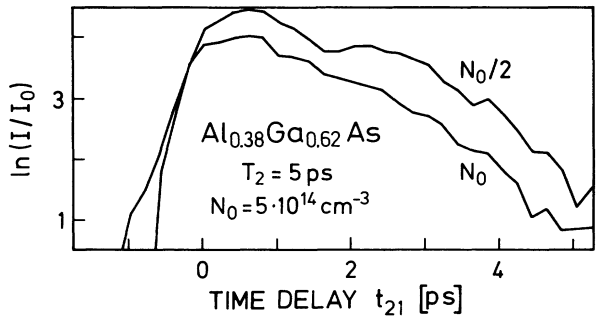

FIG. 8. Semilogarithmic plot of the time-integrated spontaneous photon echo intensity from an $Al_xGa_{1-x}As$ mixed crystal as a function of time delay t_{21}. The photoluminescence spectrum of the sample and the excitation pulse spectrum are displayed in Fig. 7. The dephasing time T_2 amounts to 5 ps for both the exciton densities N_0 and $N_0/2$ (temperature 10 K). The curves are arbitrarily shifted along the vertical axis.

are similar.

At higher densities, exciton-exciton scattering sets in and results in a decrease of the dephasing time in $Al_xGa_{1-x}As$. The onset of exciton-exciton scattering is demonstrated by the data shown in Fig. 9 where the decay of the time-integrated stimulated photon echo intensity at the density N_0 and at the density $2N_0$ is depicted in a semilogarithmic plot. The dephasing time decreases from 5 to 4 ps if the exciton density is increased from N_0 to $2N_0$. With further increasing exciton density a continuous decrease of the dephasing time is observed, indicating that exciton-exciton scattering becomes the dominant scattering mechanism in $Al_xGa_{1-x}As$ at densities higher than $2N_0 = 10^{15}$ cm^{-3}.

We have calculated the mean interparticle distance from the exciton density in order to compare the efficiency of exciton-exciton scattering in $Al_xGa_{1-x}As$ and $CdS_{1-x}Se_x$ mixed crystals. The mean interparticle

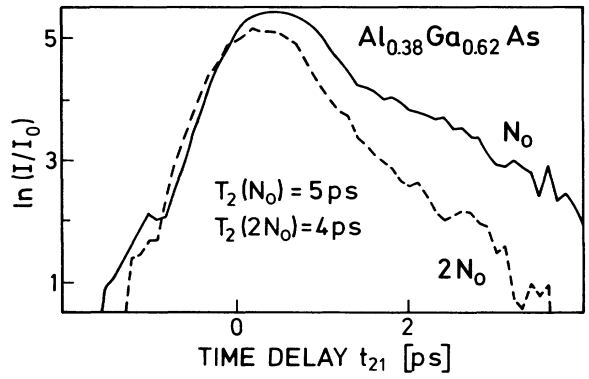

FIG. 9. Semilogarithmic plot of the time-integrated stimulated photon echo intensity from an $Al_xGa_{1-x}As$ mixed crystal as a function of time delay t_{21}. The photoluminescence spectrum of the sample and the excitation pulse spectrum are shown in Fig. 7. The dephasing time T_2 amounts to 5 ps at the exciton density $N_0 = 5\times10^{14}$ cm^{-3} (solid curve) and decreases to 4 ps at the density $2N_0$ (dashed curve). The temperature is 10 K. The curves are arbitrarily shifted along the vertical axis.

distance has been normalized to the exciton Bohr radius to account for the differences in exciton size. The normalized interparticle distance d_n is given by

$$d_n = \frac{1}{a_B}\left[\frac{3}{4\pi}\frac{1}{N_{\text{exc}}}\right]^{1/3}, \tag{13}$$

where N_{exc} is the exciton density and a_B is the Bohr radius of the exciton. The normalized interparticle distance has been calculated for excitons in $Al_xGa_{1-x}As$ at the density $2N_0$, where exciton-exciton scattering contributes to dephasing. We have also determined the normalized interparticle distance for excitons in $CdS_{1-x}Se_x$ at a density where exciton-exciton interaction is not observed. We find that the normalized interparticle distance between *interacting* excitons in $Al_xGa_{1-x}As$ is larger than the distance between *noninteracting* excitons in $CdS_{1-x}Se_x$. This result provides evidence that the localization radius of excitons in $Al_xGa_{1-x}As$ is larger than in $CdS_{1-x}Se_x$ mixed crystals. Exciton localization in $Al_xGa_{1-x}As$ can only be weak while excitons in $CdS_{1-x}Se_x$ are strongly localized.

At this point, we can only rule out strong localization of excitons in $Al_xGa_{1-x}As$. At the end of this section, we will discuss in more detail the character of the exciton state in $Al_xGa_{1-x}As$.

We now turn back to the dephasing response obtained at the exciton density N_0. Exciton-exciton scattering does not yet contribute to phase relaxation in $Al_xGa_{1-x}As$ at this density. Optical dephasing thus can only result from the population decay, i.e., energy relaxation (exciton-phonon scattering) and recombination, and from elastic scattering at the disorder potential. In order to separate the contributions of these scattering mechanisms, we have investigated the population dynamics at the density N_0.

The intensity of the three-pulse FWM signal is plotted as a function of the time delay t_{23} between pulse no. 2 and pulse no. 3 in Fig. 10. The time delay t_{21} between pulse no. 1 and pulse no. 2 is kept constant. For the lower curve, t_{21} amounts to 2.5 ps, which is larger than the pulse duration. The FWM signal at negative time delays t_{23} then originates from a grating set up by pulse no. 1 and pulse no. 3, which is probed by pulse no. 2. The decay of this signal depends on both the dephasing time T_2 and the energy relaxation time T_3 and is not evaluated any further. At positive time delays t_{23}, however, the decay of a phased array is monitored which is set up by pulse no. 1 and pulse no. 2 and probed by pulse no. 3. This decay reflects recombination, diffusion, and energy relaxation within the phased array. The upper curve in Fig. 10 is obtained for a fixed time delay $t_{21}=0$ ps, where pulse no. 1 and pulse no. 2 coincide in time. In this experiment, an ordinary population grating is set up, which only decays due to recombination and diffusion. The population grating decays with a time constant of 700 ps, demonstrating that in $Al_xGa_{1-x}As$ recombination can be neglected with respect to phase relaxation. Moreover, the decay of the phased array signal can be corrected for recombination and diffusion as the corresponding time constant is known from the population grating experiment. We are then able to determine the energy relaxation time T_3 separately. The energy relaxation time amounts to 20 ps, whereas the dephasing time of 5 ps is shorter by a factor of 4. Therefore, we are far off the limit where phase relaxation is dominated by energy relaxation. The dephasing time of 5 ps corresponds to a homogeneous linewidth of 260 μeV. The contribution of exciton-phonon interaction to the homogeneous linewidth amounts to 35 μeV as calculated from the energy relaxation time of 20 ps. Thus, exciton-phonon interaction processes only yield a small contribution to phase relaxation in $Al_xGa_{1-x}As$. A contribution to the homogeneous linewidth of 225 μeV thus has to be attributed to elastic disorder scattering. Consequently, elastic scattering at the disorder potential essentially contributes to phase relaxation in $Al_xGa_{1-x}As$ mixed crystals in contrast to the findings for $CdS_{1-x}Se_x$.

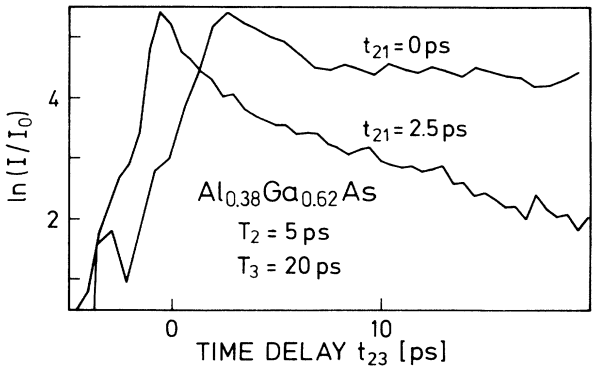

FIG. 10. Semilogarithmic plot of the time-integrated intensity of three-pulse FWM signals from $Al_xGa_{1-x}As$ as a function of time delay t_{23}. The photoluminescence spectrum of the $Al_xGa_{1-x}As$ sample and the excitation pulse spectrum are shown in Fig. 7. The upper curve is obtained for a fixed time delay $t_{21}=0$ ps and reflects the decay of a population grating. The lower curve (fixed time delay $t_{21}=2.5$ ps) shows the decay of a phased array, from which the energy relaxation time T_3 can be determined to 20 ps. All data are obtained at the exciton density $N_0=5\times10^{14}$ cm^{-3} and at a temperature of 10 K, where the dephasing time T_2 amounts to 5 ps.

On the basis of this experimental result and the theoretical considerations outlined in Sec. IV, the disorder potential in $Al_xGa_{1-x}As$ can be characterized. A fast dephasing response due to disorder is predicted if the disorder potential is short range compared to the exciton Bohr radius either in the case of a mobile exciton or in the case where the exciton is strongly localized via one of its constituents, e.g., the hole. In the case of strong hole localization, it is necessary to excite the 1s state and some of the higher states of an exciton simultaneously in order to get a fast dephasing response due to disorder. In our experiment, it is possible to fulfill this condition since the spectrum of the 1-ps pulses is broad compared to the relatively small exciton binding energy of 5–10 meV (Ref. 85) in $Al_xGa_{1-x}As$. However, it should be possible to overcome the disorder-induced contribution to dephasing by applying spectrally small pulses if the model of strong hole localization applies. In this case, the dephasing time should increase to 40 ps according to the relation $T_2=2T_3$ since the energy relaxation time amounts to 20

ps. We consequently have measured the dephasing time using pulses of 7-ps duration with a spectrum of less than 0.5-meV halfwidth. With these longer pulses the dephasing time cannot be resolved in time, i.e., the dephasing time does not significantly increase as compared to the value of 5 ps determined by spectrally broad pulses. Consequently, we can rule out the model of strong exciton localization via the localization of the hole. It follows in agreement with our earlier conclusion that exciton localization in $Al_xGa_{1-x}As$ can only be weak.

With respect to the correlation length of the random potential we note that $Al_xGa_{1-x}As$ mixed crystals have recently been investigated by scanning tunneling microscopy.[86] The length scale of inhomogeneities was found to be 10 Å. The Bohr radius of an exciton in $Al_{0.38}Ga_{0.62}As$ is roughly 80 Å.[85] Thus, scanning tunneling microscopy indicates short-range disorder, in agreement with the results from the photon echo experiments.

To conclude this section, we discuss the efficiency of exciton-phonon interaction in $Al_xGa_{1-x}As$. Exciton-phonon interaction yields a contribution of 35 μeV to the homogeneous linewidth. This is larger by about one order of magnitude as compared to $CdS_{1-x}Se_x$ mixed crystals where the considerable reduction of the exciton-phonon scattering rate is a direct result of the strong localization of excitons and the hopping dynamics in the localized regime. Thus, the comparison of exciton-phonon scattering rates in $Al_xGa_{1-x}As$ and $CdS_{1-x}Se_x$ gives further support that exciton localization in $Al_xGa_{1-x}As$ can only be weak, which has earlier been concluded from the different efficiency of exciton-exciton scattering. We can also compare dephasing rates and exciton-phonon scattering rates in $Al_xGa_{1-x}As$ mixed crystals to those of free excitons in the ordered binary compound GaAs.[61] The overall homogeneous linewidth of free excitons in GaAs is comparable to that of excitons in $Al_xGa_{1-x}As$. The exciton-phonon contribution to the homogeneous linewidth, however, is about half an order of magnitude larger in GaAs under comparable experimental conditions.[61] The different exciton-phonon scattering rates of excitons in $Al_xGa_{1-x}As$ and free excitons in GaAs show that the exciton state in $Al_xGa_{1-x}As$ mixed crystals is considerably affected by disorder. Excitons in $Al_xGa_{1-x}As$ cannot be considered as free excitations as in GaAs.

Our picture of disorder in $Al_xGa_{1-x}As$ is thus the following. Disorder has a large impact on the exciton state. Excitons in $Al_xGa_{1-x}As$ are mobile in the sense of Sec. IV, i.e., they are either delocalized or weakly localized as a whole with a localization radius larger than the exciton Bohr radius. In any case, the disorder potential contains considerably short-range fluctuations, which account for the large contribution of disorder-induced dephasing to the total dephasing rate.

VII. CONCLUSION

We have investigated optical dephasing of excitons in the disordered semiconductor mixed crystals $CdS_{1-x}Se_x$ and $Al_xGa_{1-x}As$ both experimentally and theoretically. Spontaneous and stimulated photon echo experiments in dependence of the excitation intensity, photon energy, and temperature allow us to separate the different contributions to the total dephasing rate. In particular, we can independently determine the elastic-scattering rate, which provides a basis to characterize the disorder potential and the mechanism of localization.

In $CdS_{1-x}Se_x$ the dephasing time amounts to several hundreds of picoseconds, corresponding to a homogeneous linewidth of only a few μeV. The dephasing rate is smaller by more than one order of magnitude as compared to free excitons as a result of localization. Localization considerably reduces exciton-exciton and intersite exciton-phonon scattering in $CdS_{1-x}Se_x$. We have shown that optical dephasing mainly results from the population decay, particularly from hopping processes, i.e., intersite exciton-phonon scattering. In $CdS_{1-x}Se_x$ disorder does not significantly contribute to phase relaxation.

Optical dephasing of excitons is much faster in $Al_xGa_{1-x}As$. The dephasing time amounts to 5 ps at low densities, corresponding to a homogeneous linewidth of 260 μeV. In this regime, where exciton-exciton scattering does not contribute to dephasing, the homogeneous linewidth of excitons in $Al_xGa_{1-x}As$ has two contributions: (i) exciton-phonon scattering yields a contribution of 35 μeV as calculated from the experimentally determined energy relaxation time of 20 ps and (ii) elastic scattering at the disorder potential results in a homogeneous broadening of the exciton line of 225 μeV and gives the main contribution to dephasing. The different dephasing behavior of excitons in $CdS_{1-x}Se_x$ and $Al_xGa_{1-x}As$ is related to the different microscopic properties of disorder in the respective mixed crystals. In particular, our results indicate that the disorder potential in $Al_xGa_{1-x}As$ is short range as compared to the exciton Bohr radius.

The overall homogeneous linewidth in $Al_xGa_{1-x}As$ is comparable to that of free excitons in GaAs,[61] yet the ratio of the different contributions to dephasing is different in ordered GaAs and $Al_xGa_{1-x}As$ mixed crystals. Compared to the ordered GaAs, exciton-phonon scattering in $Al_xGa_{1-x}As$ is reduced, indicating that the disorder significantly affects the exciton state. The smaller exciton-phonon scattering rate is compensated for by the additional elastic alloy scattering.

In $CdS_{1-x}Se_x$ and $Al_xGa_{1-x}As$ different degrees of exciton localization are revealed by the efficiency of exciton-exciton and exciton-phonon scattering. Exciton-exciton scattering does not contribute to phase relaxation at low and at intermediate densities in $CdS_{1-x}Se_x$, demonstrating rather strong exciton localization. In $Al_xGa_{1-x}As$ mixed crystals strong localization of excitons can be ruled out. Exciton-exciton interaction contributes at intermediate densities in $Al_xGa_{1-x}As$ while it is unimportant only in the low-density regime.

In conclusion, the nonlinear optical response of a semiconductor mixed crystal critically depends on the detailed nature of disorder. For $CdS_{1-x}Se_x$ and $Al_xGa_{1-x}As$ mixed crystals we have shown that photon echo experiments are an appropriate tool to characterize disorder and localization in semiconductors. It should be possible to extend this approach to other semiconductor

bulk crystals as well as to semiconductor microstructures.

ACKNOWLEDGMENTS

We are indebted to K. Ploog, Stuttgart, W. Stolz, Marburg, and S. G. Shevel, Kiev, for providing us with the $Al_xGa_{1-x}As$ and $CdS_{1-x}Se_x$ samples, respectively. Many helpful discussions with S. Schmitt-Rink and J. Feldmann as well as the expert technical assistance of M. Preis are gratefully acknowledged. This work has been supported financially by the Deutsche Forschungsgemeinschaft.

[1]P. W. Anderson, Phys. Rev. **109**, 1492 (1958).
[2]L. Bányai, in *Physique de Semiconducteurs,* edited by M. Hulin (Dunod, Paris, 1964), p. 417.
[3]H. Müller and P. Thomas, Phys. Rev. Lett. **51**, 702 (1983).
[4]H. Müller and P. Thomas, J. Phys. C **17**, 5337 (1984).
[5]H. Overhof and P. Thomas, *Electronic Transport in Hydrogenated Amorphous Semiconductors,* Springer Tracts in Modern Physics Vol. 114 (Springer, Heidelberg, 1989).
[6]J. A. Kash, A. Ron, and E. Cohen, Phys. Rev. B **28**, 6147 (1983).
[7]S. Shevel, R. Fischer, G. Noll, E. O. Göbel, P. Thomas, and C. Klingshirn, J. Lumin. **37**, 45 (1987).
[8]C. Gourdon, P. Lavallard, S. Permogorov, A. Reznitsky, Y. Aaviksoo, and Y. Lippmaa, J. Lumin. **39**, 111 (1987).
[9]C. Gourdon and P. Lavallard, Phys. Status Solidi B **153**, 641 (1989).
[10]Ch. Lonsky, P. Thomas, and A. Weller, Phys. Rev. Lett. **63**, 652 (1989).
[11]C. Lonsky, P. Thomas, and A. Weller, J. Lumin. **45**, 77 (1990).
[12]D. Bennhardt, P. Thomas, A. Weller, M. Lindberg, and S. W. Koch, Phys. Rev. B **43**, 8934 (1991).
[13]H. Haug and S. Schmitt-Rink, Prog. Quantum Electron. **9**, 3 (1984).
[14]S. Schmitt-Rink and D. S. Chemla, Phys. Rev. Lett. **57**, 2752 (1986).
[15]S. Schmitt-Rink, D. S. Chemla, and H. Haug, Phys. Rev. B **37**, 941 (1988).
[16]M. Lindberg and S. W. Koch, Phys. Rev. B **38**, 3342 (1988).
[17]S. Schmitt-Rink, D. S. Chemla, and D. A. B. Miller, Adv. Phys. **38**, 89 (1989).
[18]I. Balslev, R. Zimmermann, and A. Stahl, Phys. Rev. B **40**, 4095 (1989).
[19]H. Haug and S. W. Koch, *Quantum Theory of the Optical and Electronic Properties of Semiconductors* (World Scientific, Singapore, 1990).
[20]R. Binder, S. W. Koch, M. Lindberg, N. Peyghambarian, and W. Schaefer, Phys. Rev. Lett. **65**, 899 (1990).
[21]R. Binder, S. W. Koch, M. Lindberg, W. Schaefer, and F. Jahnke, Phys. Rev. B **43**, 6520 (1991).
[22]J. M. Hvam, C. Dörnfeld, and H. Schwab, Phys. Status Solidi B **150**, 387 (1988).
[23]C. Dörnfeld and J. M. Hvam, IEEE J. Quantum Electron. **25**, 904 (1989).
[24]L. Schultheis, J. Kuhl, A. Honold, and C. W. Tu, Phys. Rev. Lett. **57**, 1635 (1986).
[25]L. Schultheis, J. Kuhl, A. Honold, and C. W. Tu, Phys. Rev. Lett. **57**, 1797 (1986).
[26]B. Segall and D. T. F. Marple, in *Physics and Chemistry of II-IV-Compounds,* edited by M. Aven and J. S. Prener (North-Holland, Amsterdam, 1967).
[27]C. Klingshirn and H. Haug, Phys. Rep. **70**, 315 (1981).
[28]Joseph L. Birman, Phys. Rev. **114**, 1490 (1959).
[29]Landolt-Börnstein: Numerical Data and Functional Relationships in Science and Technology, New Series, Group III, Vol. 17b, edited by O. Madelung (Springer, Berlin, 1982).
[30]O. Goede, L. John, and D. Hennig, Phys. Status Solidi B **89**, K183 (1978).
[31]E. Cohen and M. D. Sturge, Phys. Rev. B **25**, 3828 (1982).
[32]S. Permogorov, A. Reznitskii, S. Verbin, G. O. Müller, P. Flögel, and M. Nikiforova, Phys. Status Solidi B **113**, 589 (1982).
[33]F. A. Majumder, S. Shevel, V. G. Lyssenko, H. E. Swoboda, and C. Klingshirn, Z. Phys. B **66**, 409 (1987).
[34]B. I. Halperin and M. Lax, Phys. Rev. **148**, 722 (1966).
[35]S. D. Baranovskii and A. L. Efros, Fiz. Tekh. Poluprovodn. **12**, 2233 (1978) [Sov. Phys. Semicond. **12**, 1328 (1978)].
[36]A. G. Abdukadyrov, S. D. Baranovskii, S. Yu. Verbin, E. L. Ivchenko, A. Yu. Naumov, and A. Reznitskii, Zh. Eksp. Teor. Fiz. **98**, 2056 (1990) [Sov. Phys. JETP **17**, 1155 (1990)].
[37]S. Permogorov and A. Reznitsky, J. Lumin. (to be published).
[38]S. Permogorov, A. Reznitsky, S. Verbin, and V. Lyssenko, Solid State Commun. **47**, 5 (1983).
[39]G. Wicks, W. I. Wang, C. E. C. Wood, L. F. Eastman, and L. Rathbun, J. Appl. Phys. **52**, 5792 (1981).
[40]W. T. Tsang and V. Swaminathan, Appl. Phys. Lett. **39**, 486 (1981).
[41]J. R. Shealy, V. G. Kreismanis, D. K. Wagner, and J. M. Woodall, Appl. Phys. Lett. **42**, 83 (1983).
[42]M. Heiblum, E. E. Mendez, and L. Osterling, J. Appl. Phys. **54**, 6982 (1983).
[43]E. F. Schubert, E. O. Göbel, Y. Horikoshi, K. Ploog, and H. J. Queisser, Phys. Rev. B **30**, 813 (1984).
[44]H. Jung, A. Fischer, and K. Ploog, Appl. Phys. A **33**, 9 (1984).
[45]D. C. Reynolds, K. K. Bajaj, C. W. Litton, P. W. Yu, J. Klem, C. K. Peng, H. Morkoç, and J. Singh, Appl. Phys. Lett. **48**, 727 (1986).
[46]S. M. Olsthoorn, F. A. J. M. Driessen, and L. J. Giling, Appl. Phys. Lett. **58**, 1274 (1991).
[47]H. C. Casey and M. B. Panish, *Heterostructure Lasers* (Academic, New York, 1978).
[48]J. Singh and K. K. Bajaj, Appl. Phys. Lett. **44**, 1075 (1984).
[49]J. Singh and K. K. Bajaj, Appl. Phys. Lett. **48**, 1077 (1986).
[50]S. M. Lee and K. K. Bajaj, Appl. Phys. Lett. **60**, 853 (1992).
[51]M. D. Sturge, E. Cohen, and R. A. Logan, Phys. Rev. B **27**, 2362 (1983).
[52]*Ultrashort Laser Pulses and Applications,* edited by W. Kaiser, Topics in Applied Physics Vol. 60 (Springer, Berlin, 1988).
[53]A. M. Weiner, S. De Silvestri, and E. P. Ippen, J. Opt. Soc. Am. B **2**, 654 (1985).
[54]H. J. Eichler, P. Günther, and D. W. Pohl, *Laser-Induced Dynamic Gratings,* Springer Series in Optical Sciences Vol. 50 (Springer, Berlin, 1986).
[55]T. Yajima and Y. Taira, J. Phys. Soc. Jpn. **47**, 1620 (1979).
[56]N. A. Kurnit, I. D. Abella, and S. R. Hartmann, Phys. Rev. Lett. **13**, 567 (1964).
[57]I. D. Abella, N. A. Kurnit, and S. R. Hartman, Phys. Rev. **141**, 391 (1966).
[58]P. Hu, S. Geschwind, and T. M. Jedju, Phys. Rev. Lett. **37**,

1357 (1976).
[59]K. Duppen, L. W. Molenkamp, and D. A. Wiersma, Physica **127B**, 349 (1984).
[60]L. W. Molenkamp and D. A. Wiersma, Phys. Rev. B **32**, 8108 (1985).
[61]Jürgen Kuhl, Alfred Honold, Lothar Schultheis, and Charles W. Tu, in *Festkörperprobleme 29 (Advances in Solid State Physics)* (Vieweg, Braunschweig, 1989).
[62]P. C. Becker, H. L. Fragnito, C. H. Brito Cruz, R. L. Fork, J. E. Cunningham, J. E. Henry, and C. V. Shank, Phys. Rev. Lett. **61**, 1647 (1988).
[63]L. Schultheis, J. Kuhl, A. Honold, and C. W. Tu, Phys. Rev. B **34**, 9027 (1986).
[64]L. Schultheis, M. D. Sturge, and J. Hegarty, Appl. Phys. Lett. **47**, 995 (1985).
[65]A. Honold, L. Schultheis, J. Kuhl, and C. W. Tu, Phys. Rev. B **40**, 6442 (1989).
[66]M. D. Webb, S. T. Cundiff, and D. G. Steel, Phys. Rev. Lett. **66**, 934 (1991).
[67]M. D. Webb, S. T. Cundiff, and D. G. Steel, Phys. Rev. B **43**, 12 658 (1991).
[68]W. Huhn and A. Stahl, Phys. Status Solidi B **124**, 167 (1984).
[69]A. Stahl and I. Balslev, *Electrodynamics of the Semiconductor Band Edge,* Springer Tracts in Modern Physics Vol. 110 (Springer, Heidelberg, 1987).
[70]M. Wegener, D. S. Chemla, S. Schmitt-Rink, and W. Schaefer, Phys. Rev. A **42**, 5675 (1990).
[71]W. Schaefer, F. Jahnke, and S. Schmitt-Rink, Phys. Rev. B (to be published).
[72]M. Lindberg, R. Binder, and S. W. Koch, Phys. Rev. A **45**, 1865 (1992).
[73]K. Leo, M. Wegener, J. Shah, D. S. Chemla, E. O. Göbel, T. C. Damen, S. Schmitt-Rink, and W. Schaeffer, Phys. Rev. Lett. **65**, 1340 (1990).
[74]P. A. Lee and T. V. Ramakrishnan, Rev. Mod. Phys. **57**, 287 (1985).
[75]D. Bennhardt, V. Heuckeroth, and P. Thomas (unpublished).
[76]Y. Yan and S. Mukamel, J. Chem. Phys. **94**, 179 (1991).
[77]C. B. Duke and G. D. Mahan, Phys. Rev. **139**, A1965 (1965).
[78]T. Takagahara, Phys. Rev. B **31**, 6552 (1985).
[79]D. Monroe, Phys. Rev. Lett. **54**, 146 (1985).
[80]D. Ouadjaout and Y. Marfaing, Phys. Rev. B **41**, 12 096 (1990).
[81]A. Miller and E. Abrahams, Phys. Rev. **120**, 745 (1960).
[82]H. Schwab and C. Klingshirn, Phys. Rev. B **45**, 6938 (1992).
[83]H. Stolz, V. Langer, E. Schreiber, S. Permogorov, and W. von der Osten, Phys. Rev. Lett. **67**, 679 (1991).
[84]H. Schwab, V. G. Lyssenko, and J. M. Hvam, Phys. Rev. B **44**, 3999 (1991).
[85]Sadao Adachi, J. Appl. Phys. **58**, R1 (1985).
[86]H. Salemink and O. Albrektsen, J. Vac. Sci. Technol. B **9**, 779 (1991).